2015 Workshop on Research, Education and Development of
Unmanned Aerial Systems (RED-UAS)
November 23-25, 2015. Cancun, Mexico

Modeling and Experimental Parameter Identification of a Multicopter via a Compound Pendulum Test Rig

Elisa Capello[1], Hyeongjun Park[2], Bruno Tavora[2],
Giorgio Guglieri[1], and Marcello Romano[2]

Abstract— **In this paper, a method to identify parameters of a multicopter is proposed via a compound pendulum test rig and data from an optical position tracking system. Moments of inertia and thrust parameters of a hexacopter are evaluated. In addition, a specific method is introduced to identify the torque by a propeller using a floating test bed. Then, nonlinear dynamic model is derived based on the obtained parameters. To verify the identification method, simulation results using the nonlinear model are compared with experimental results from flight tests.**

I. INTRODUCTION

Multicopters have been received a significant interest in various applications such as rescue missions, inspection of structures, environment monitoring, and military reconnaissance [1], [2]. Advantages of multicopters on mechanical simplicity and high maneuverability enable to conduct advanced missions in academic research and industrial applications with advanced control algorithms. A multicopter is a nonlinear, mulivariable, underactuated, and unstable system [2]. Therefore, it is important to understand and obtain a precise model of a multicopter for advanced controllers in order to execute sophisticate missions.

Researchers have studied to seek methods in identifying parameters of multicopter systems. An overview of methods for identification of quadrotors is provided in [2]. The methods on multicopter system identification are mainly divided into two different approaches: (i) direct computation of geometry and (ii) analysis from flight data [3]. For instance, CAD models are used to calculate all the missing parameters and the moment of inertia in [1], [4] for direct computation of geometry. In [1], [3], Unscented Kalman Filter (UKF) is implemented to identify and estimate parameters of quadrotors from flight data. Reference [5] suggested prediction error method (PEM) to estimate unknown parameters which minimizes a quadratic criterion applied to the prediction error using flying data near to hovering point.

Although the identification methods have used in some cases successfully, there are disadvantages in both approaches. For example, the approach of direct computation of geometry causes a computation load for mathematical and physical calculations [3]. On the other hand, the identification approach by analyzing from flight data is more accurate and computationally simpler; however, it is necessary to fly a multicopter before understand its physical characteristics exactly. Hence, there are possibilities to occur damage on the multicopter during fight tests.

In this paper, we propose a method to identify parameters of a multicopter using a compound pendulum method [6], [7] and an optical position tracking system (Vicon), avoiding complicated computations of geometry data and the risk of flight tests. Rules of compound pendulum and measures from Vicon system are employed for the evaluation of moments of inertia of thrust of a hexacopter. In addition, an *ad hoc* method is proposed to identify the system torque based on experiments with a floating spacecraft test-bed. Then, a nonlinear model is derived starting from the obtained parameters, and the effectiveness of the proposed method is evaluated comparing the simulation results with flight test data.

The paper is organized as follows. In Section II,

[1]E. Capello and G. Guglieri are with the Department of Mechanical and Aerospace Engineering, Politecnico di Torino, Torino, 10129, Italy elisa.capello@polito.it; giorgio.guglieri@polito.it

[2]H. Park, B. Tavora, and M. Romano are with the Mechanical and Aerospace Engineering Department, Naval Postgraduate School, Monterey, CA 93943, USA hpark1@nps.edu; bgrugelf@nps.edu; mromano@nps.edu

we describe a hexacopter and its characteristics. In Section III, the identification method is introduced and applied to identify the parameters of the hexacopter. The nonlinear dynamic model of the hexacopter is derived in Section IV. We provides the results of simulation using the nonlinear model and evaluate the effectiveness of the method by comparing to the experimental results in Section V. Finally conclusions are summarized in Section VI.

II. MODEL DESCRIPTION

The problem of identification proposed in this paper is applied to a multicopter with six engines. We assume that the hexacopter structure is rigid. The hexacopter consists of six arms all connected symmetrically to the central hub to simplify the balance of the separate thrusters. At the end of each arm a propeller driven by an electric motor is attached. See Fig. 1 for the hexarotor system. The center of mass (CoM) is not exactly coincident with the center of geometry (CoG). Due to the location of a battery and power regulator part, the CoM is located at $(-0.015, 0, 0)$ m in the body reference frame where the CoG is the origin. All the propellers have fixed pitch blades. As indicated in Fig. 1, three propellers rotate anticlockwise and three clockwise.

Four basic movements are considered varying the thrust produced by each propellers. The rotation of the rotors produce also a reaction torque, opposite of the rotation direction. Since half of the propellers are spinning in one direction, the net torque is zero when all rotors have equal speed.

The main control of the hexacopter is the throttle. It is used for the movements in the body vertical direction. Since the propellers are fixed pitched, the direction of the throttle is fixed and it is used to counter act the gravity. When increasing (decreasing) the throttle, the hexarotor will travel upwards (downwards). Throttle is produced by increasing (decreasing) the speed of all rotors equally. The second basic movement is related to the roll variation is produced by increasing (decreasing) the speed of rotors on right side while decreasing (increasing) the left side rotor speed of the same amount. The third movement is the pitch variation produced by increasing (decreasing) the rear rotor speed while decreasing (increasing) the front rotor speed. The yaw movement (fourth basic movement) is produced by increasing (decreasing) the speed of the rotors rotating clockwise while decreasing (increasing) the rotors rotating anticlockwise.

The electric engines are the T-Motor KV 750 (MT2212) with E-prop carbon propellers. The transmitter is the radio controller Spektrum DX7s. It is used to control the hexarotor by sending reference values for controls. The hexacopter is able to perform autonomous flight thanks to the on board installation of an autopilot, 3DR Pixhawk, that is a high-performance autopilot-on-module. Its main characteristics comprehend an open architecture, the possibility to be reprogrammed in flight and real time telemetry. The CPU is the 32 bit STM32F427 Cortex M4 core with FPU and 2Mb flash memory and 256kb of RAM with a CPU clock of 168 MHz. The autopilot is placed on the central hub together with a Lithium Polymer (LiPo) battery and the receiver connected to the ground control station. The characteristics of the hexacopter are in Table I. The total weight of the multi rotor is 1189 g.

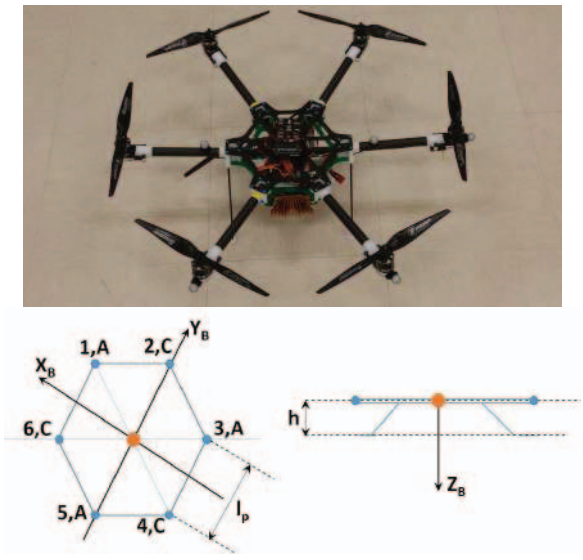

Fig. 1. From top to bottom and left to right: Hexacopter, rotation directions of motors, and reference frame. A and C represent anticlockwise and clockwise, respectively. (X_B, Y_B, Z_B) is the body reference frame.

TABLE I

HEXACOPTER CHARACTERISTICS

Part	Description	Weight
Electric motor	T-Motor KV 750 (MT2212)	$m_e = 55$ g
Propeller E-Prop	$254\ mm \times 120\ mm$	$m_p = 12$ g
LiPo Battery and power regulator	Thunder Power $1800\ mAh$	$m_b = 269$ g
Structure weight	-	$m_s = 350$ g
Total weight	-	$m = 1189$ g

III. IDENTIFICATION OF THE HEXACOPTER

The identification of multirotors systems is usually carried out with two different ways. One is based on the identification of physical parameters and the second is based on the variation of control inputs (called direct approach). Both ways are model-dependent approaches, even if once performed on one system it can easily be repeated on other systems. The most tested approach is the identification of physical parameters such as moments of inertia and the relation between propeller thrust/torque and propeller angular speed. This approach was studied by [8], [9]. The other approach is the black box identification between the virtual control input and the angular rate. References [10], [11] attempted the second approach. The drawback of the second approach is that to perform the flight experiments to acquire identification data, the multirotor has to have a working controller. This means that the input signal will not be the one actually controlling the multirotor, but a reference signal to the control system or an overlay on the controller output.

To implement the selected controller, an open loop identification method is chosen which is identification of physical parameters. The novelty of the proposed approach is the use of a Vicon system for measuring the moments of inertia and for evaluating the static gains of the engine (both thrust and torque gains). This second approach is also chosen for reducing the time of collecting data and to avoid the risk of accidents during flight tests considering that a stable and robust controller is not yet implemented on-board.

The Vicon system is a state-of-the-art infrared marker-tracking system that offers millimeter resolution of three-dimensional (3D) spatial displacements. Ten Vicon cameras (see Fig. 12) are installed along the walls of the laboratory to collect and stream high quality, 3D position and attitude information. The Vicon server is able to provide the position and the attitude of a rigid body with a resolution between 0.001 and 0.01 mm. The resolution depends on the distance and number of passive markers on the tracked body.

A. Identification of Moments of Inertia

For the evaluation of the moments of inertia of a body, masses and spatial distributions of the components are measured in the direct computation of geometry approach. All the distances are measured and all the components have to be weighted. One problem of the geometric evaluation of the moments of inertia is that the body has to be assembled or disassembled in the laboratory. If a commercial multirotor is considered, disassembling the overall system should be time consuming.

In this research, the idea is to use the rules of compound pendulum [12] for evaluating the moments of inertia of the body. It is also a prototypical system for demonstrating the Lagrangian and Hamiltonian approaches to dynamics and the machinery of nonlinear dynamics.

The equations of motion are derived by Lagrangian dynamics,

$$\mathcal{L} = K - V, \tag{1}$$

where K and V are the kinetic and potential energy of the pendulum, respectively. We assume that the total energy E at the initial time t_0 is equal to the

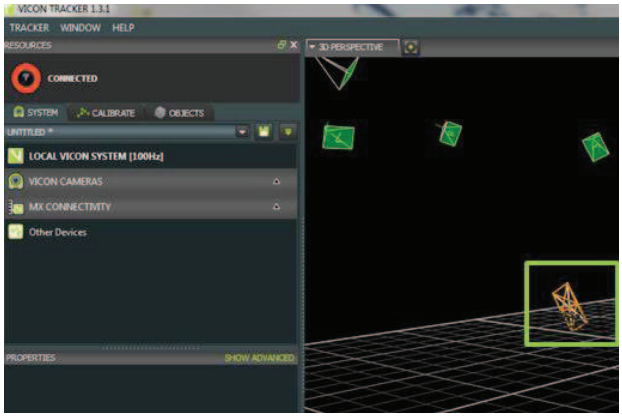

Fig. 2. Hexacopter and cameras captured by Vicon system

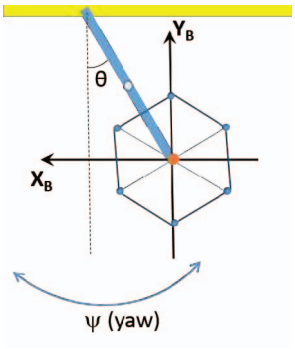

Fig. 3. Compound pendulum setup for the evaluation of the yaw moments of inertia

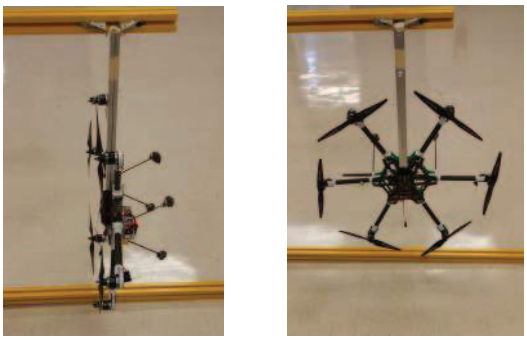

Fig. 4. Pendulum experimental setup for the evaluation of the yaw moments of inertia (left) and of the pitch moments of inertia (right)

maximum potential energy V and that the kinetic energy is zero. The mass and geometry of the system are known. The variation of the angle θ (inclination of the pendulum, see Fig. 3) is known at each time step and evaluated with the Vicon system.

The unknown moments of inertia, directly evaluated with the Vicon system and pendulum theory, are the moments around the Z_B (left of Fig. 4) and Y_B (right of Fig. 4) axes. As shown in Fig. 4 the setup of the experiments is the following:

- A rigid rod is connected to the hexacopter by a system of screws and nuts,
- The same rod is connected to a structure with a base on ground.

The Lagrangian approach is applied to the pendulum. The setup of the experiments is in Fig. 5.

The kinetic and potential energy can be defined as follows

$$K = \tfrac{1}{2}(m_1 l_1^2 + m(l_1 + d)^2 + I_{rod} + I)\dot{\theta}^2, \quad (2)$$

$$V = m_1 g(1 - l_1 \cos\theta) + mg(1 - (l_1 + d)\cos\theta), \quad (3)$$

where l_1 is the distance between the joint point on the yellow bar and the CoG of the rod, d is the distance between the CoG of the rod and the CoM of the hexacopter, m is the hexacopter mass, m_1 is the rod mass, and θ is the pendulum inclination angle. I_{rod} is the moment of inertia of the bar. It is easily evaluated from the rules of parallelepiped inertia starting from the known data of weight and geometry. I_{rod_x}, I_{rod_y}, and I_{rod_z} are 0.0071, 2.948×10^{-5}, and 0.0071 [kgm^2], respectively. I is the unknown hexacopter moment of inertia. The angle θ, as in the previously cases, is evaluated by the Vicon. Applying the Lagrangian equation,

$$\frac{d}{dt}\frac{\partial K}{\partial \dot{\theta}} + \frac{\partial V}{\partial \theta} = 0, \quad (4)$$

with $\frac{\partial K}{\partial \dot{\theta}} = A\dot{\theta}$ and $\frac{\partial V}{\partial \theta} = B\sin\theta$. For small angle of inclination, the natural frequency of oscillation can be evaluated as

$$\omega^2 = \frac{B}{A}, \quad (5)$$

where ω is the natural frequency.

From the measurement by the Vicon system, the period of oscillation of the pendulum is known and can be easily evaluated from the analysis of the time history. The time histories are in Fig. 6. The period of oscillation for the yaw angle (I_{zz} evaluation) is $T_z = 1.4260$ s and for the pitch angle (I_{yy} evaluation) is $T_y = 1.3909$ s.

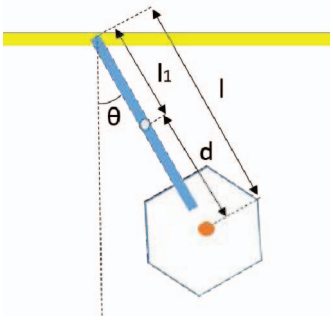

Fig. 5. Setup for the Lagrangian approach

In detail, we have

$$T_{\text{hexa}} = \frac{2\pi}{\omega} = \frac{2\pi}{\sqrt{\frac{B}{A}}}, \tag{6}$$

with T_{hexa} period of oscillation, and

$$\begin{aligned} I &= \frac{T^2}{4\pi^2}\left(m_1 g\tfrac{l_1}{2} + mg(l_1+d)\right) - m_1\tfrac{l_1^2}{4} \\ &\quad - m(l_1+d)^2 - I_{rod}. \end{aligned} \tag{7}$$

I_{yy} and I_{zz} are obtained as 0.0254 kgm^2 and 0.0418 kgm^2, respectively. Similarly, I_{xx} is obtained as 0.0286 kgm^2.

B. Identification of Engine Characteristics

The thrust and aerodynamic torque produced by a propeller are related to the rotational velocity of the propeller blade. The main idea of the identification of the engine is to derive a simplified relation of the thrust generation model as in [13]. If the rotational velocity of propeller i is denoted Ω_i, then the generated thrust T_i is

$$T_i = k_T \Omega_i^2, \tag{8}$$

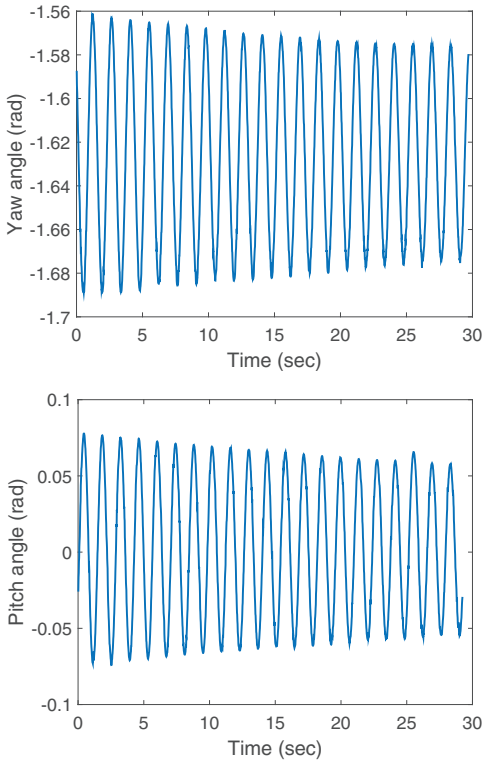

Fig. 6. Time histories of the yaw and pitch angles

Fig. 7. Setup for the thrust experiments

where $i = 1, \ldots, 6$, and k_T is a propeller specific constant. In the same way, the aerodynamic torque C_i of propeller i becomes

$$C_i = k_Q \Omega_i^2. \tag{9}$$

where k_Q is a propeller specific constant for torque experiments.

The thrust constant k_T defines the relationship between the steady state thrust generated by the engines when hovering and by the angular velocity of the rotors. The hexacopter is fixed to a solid bar as a pendulum (see Fig. 7) and only one propeller is mounted. In Fig. 8, the thrust is obtained from the following equilibrium of moments around the joint point,

$$m_1 l_1 g \sin\theta + mgl_2 \sin\theta - Tl = 0, \tag{10}$$

where m_1 is the rod mass, l_1 is the distance between the joint point on the yellow bar and the CoG of the rod, m is the hexacopter total mass, l_2 is the distance between the joint point on the yellow bar and the hexacopter CoG, l is the distance between the joint of the rod and the application point of the thrust, and T is the thrust of the single motor.

Different experiments are performed at different Pulse Width Modulation (PWM) inputs to the motors. In that way an analytical relationship between the thrust T and the PWM signal can be derived.

The input signal is in PWM which is generated by the Pixhawk and has a limited boundary from 1100 µs to 1900 µs. The motors have no response in the case of PWM values smaller than the lower

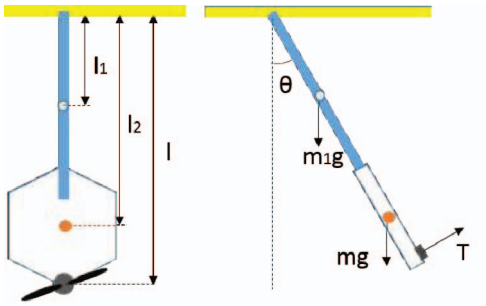

Fig. 8. Scheme for the thrust experiments

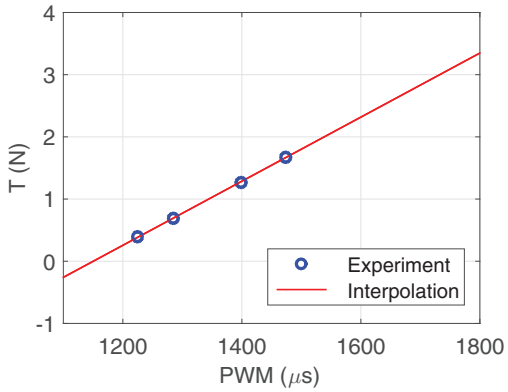

Fig. 9. Thrust variation with respect to PWM measures

limit. On the other hand, a saturation phenomenon occurs for values larger than the upper limit of PWM. The final relationship between PWM and thrust considering a linear interpolation from the experimental data is

$$T = 0.0052P - 5.9266, \tag{11}$$

where P is the value of PWM [μs] as shown in Fig. 9. The thrust constant k_T in (8) is 1.2736×10^{-7} [Ns^2] based on the relation between the PWM signals and the rotational speed of each rotor in Revolutions Per Minute (RPM) in Fig. 10.

The torque constant k_Q relates the rotational speed of each rotors in idle position to the torque produced by the rotor with respect to the motor axis. To find an estimate of this constant, we use a frictionless system based on experiments performed on a granite rig with floating spacecraft. See Fig. 11 for the experiment setup. The hexarotor is mounted on a spacecraft robot [14], [15] developed in the Space Robotics Laboratory at Naval Postgraduate School (see Fig. 11).

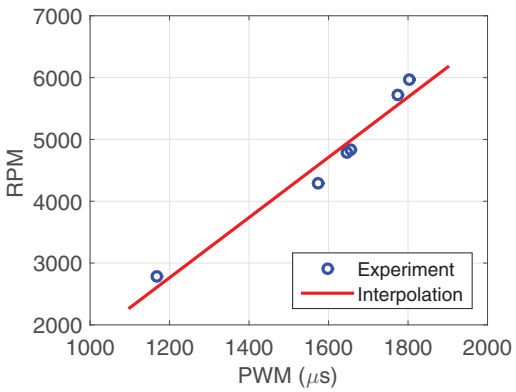

Fig. 10. Relation between the rotational speed of a rotor and PWM measures

The main floating surface is a granite monolith with the following characteristics:

- Dimensions: 4 m × 4 m × 0.3 m
- Surface precision grade: AAA
- Planar accuracy: $\pm 0.127 \times 10^{-2}$ mm
- Horizontal leveling precision: < 0.01 deg
- Mass: 15.2 × 103 kg .

The testbed is also provided with:

- Linux Real-Time work station
- Ad-Hoc WiFi internal network for data streaming
- High pressure air compressor and compressed air filling station.

Three propellers rotating in the same direction are mounted on the hexacopter. The spacecraft is floating on the granite rig with four thrusters on. Experiments of two cases are performed:

1) no propellers of the hexacopter switched on and four thrusters of the spacecraft robot

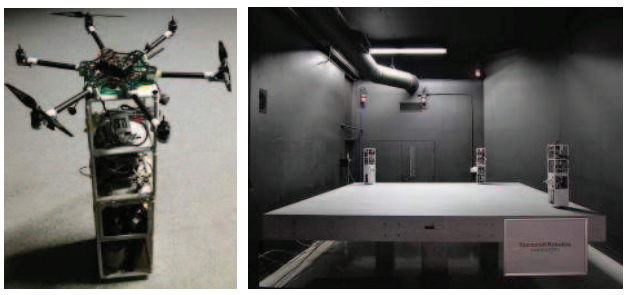

Fig. 11. Testbed setup for torque experiments (left) and the floating spacecraft simulator testbed at Spacecraft Robotics Laboratory (right)

switched on for 5 s,

2) only three propellers of the hexacopter switched on.

The torque is assumed to be constant for all the experiments with propellers switched off. The Vicon measures in the first case are in Fig. 12.

In general, the torque τ is measured starting from the Newton's second law

$$\tau = I_z \dot{\omega}_{prop}, \tag{12}$$

where I_z moments of inertia along the Z-axis of the system of Fig. 11 (moments of inertia of the system of spacecraft robot and the hexacopter). $\dot{\omega}_{prop}$ is the angular velocity of the whole body. The experiments of the propellers off case are performed for the evaluation of the moment of inertia of the body I_z since the torque is constant,

$$\tau_0 = 2 d_T F, \tag{13}$$

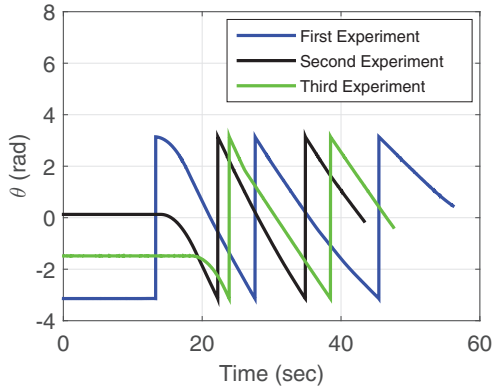

Fig. 12. Vicon measures for experiment of no propellers switched on

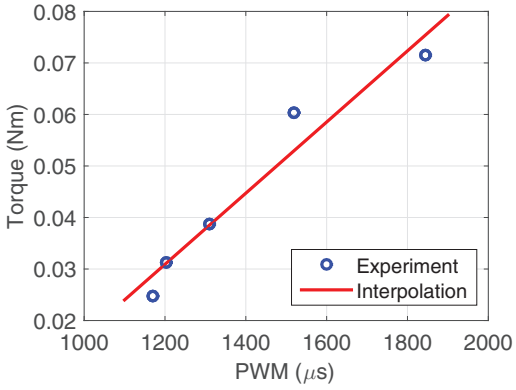

Fig. 13. Torque variation with respect to PWM measures

where τ_0 is the measured torque with the propellers off, d_T is the distance between two thrusters, and $F = 0.15$ [N] is the force produced by the four thrusters. In our case, τ_0 is known and equal to 0.0030 [Nm]. From the Vicon data, we obtain $\dot{\omega}_{prop}$ and compute I_z in Case 1. Since we now know I_z, the torque by the three propellers are obtained using Vicon data from the experiments in Case 2.

The final relationship between PWM and torque

$$\tau = 0.0001P - 0.0520,$$

considering a linear interpolation between the experimental data. The obtained curve is in Fig. 13. The torque constant k_Q in (9) is obtained as 2.4325×10^{-9} [Nms^2].

IV. NONLINEAR MODEL

In this section, we derive a nonlinear dynamic model of the hexacopter using the obtained parameters. The motion of a rigid body can be decomposed into the translational and rotational components. In order to describe the dynamics of the hexacopter assumed to be a rigid body, the Newton-Euler equations [16] are taken into account. Different nonlinear models for hexacopters are introduced in [17], [18]. Nine equations of motion are here considered: (i) three equations for the translational velocity with components $(u, v, w)^T$, (ii) three equations for angular velocities $(p, q, r)^T$ and (iii) three angles $(\phi, \vartheta, \psi)^T$ for the orientation. For the translational and angular velocity, we have

$$F_B = m\frac{dV}{dt} + \omega_B \times V, \tag{14}$$

$$M_B = I\dot{\omega}_B + \omega_B \times (I\omega_B) + I_p \omega_B \times \Omega, \tag{15}$$

where $F_B \in \mathbb{R}^3$ and $M_B \in \mathbb{R}^3$ are the total forces and moments acting on the hexacopter, respectively. $V = (u, v, w)^T \in \mathbb{R}^3$ is the translational velocity, $\omega_B = (p, q, r)^T \in \mathbb{R}^3$ is the angular velocity, $I = diag(I_{xx}, I_{yy}, I_{zz}) \in \mathbb{R}^{3\times3}$ is the inertia matrix (diagonal due to the hexacopter symmetry) with respect to the body axes. I_p is the moment of inertia about the propeller axis and is obtained as $\frac{1}{2}m_p r^2$ where m_p is the mass and r is the radius of the propeller. Ω is expressed as $-\Omega_1 + \Omega_2 - \Omega_3 + \Omega_4 - \Omega_5 + \Omega_6$, considering the rotating direction of the propellers where Ω_i, $i = 1, \ldots, 6$ is the

$$\dot{\phi} = p + q\sin\phi\tan\vartheta + r\cos\phi\tan\vartheta, \quad (16)$$
$$\dot{\vartheta} = q\cos\phi - r\sin\phi, \quad (17)$$
$$\dot{\psi} = \frac{q\sin\phi}{\cos\vartheta} + \frac{r\cos\phi}{\cos\vartheta}, \quad (18)$$
$$\dot{u} = qw - rv + g\sin\vartheta, \quad (19)$$
$$\dot{v} = pw + ru - g\cos\vartheta\sin\phi, \quad (20)$$
$$\dot{w} = pv - qu - g\cos\vartheta\cos\phi - \frac{\sum_{i=1}^{6} T_i}{m}, \quad (21)$$
$$\dot{p} = \frac{1}{I_{xx}}[(T_4 + T_6 - T_1 - T_3)d_1 + (T_5 - T_2)l_p + qr(I_{yy} - I_{zz}) - I_p q\Omega], \quad (22)$$
$$\dot{q} = \frac{1}{I_{yy}}[(T_1 + T_6)(d_2 + d_3) - (T_3 + T_4)(d_2 - d_3) + (T_2 + T_5)d_3 + pr(I_{zz} - I_{xx}) + I_p p\Omega], \quad (23)$$
$$\dot{r} = \frac{1}{I_{zz}}[(C_1 - C_2 + C_3 - C_4 + C_5 - C_6) + pq(I_{xx} - I_{yy})]. \quad (24)$$

angular velocity of each propellers. All quantities are expressed in the body fixed frame.

The attitude of the body is described by three Euler angles. The variation of the Euler angles $(\phi, \vartheta, \psi)^T$, which is defined by the kinematic equations, can be obtained as in (16), (17), and (18).

The forces and torques acting on the hexacopter are gravity, aerodynamic forces, and torques produced by the propellers and the gyroscopic effects from the rotation of the propellers. The torque caused by the angular acceleration of the propeller has been neglected. The air frames movement through the air will cause friction. For the hexacopter this force is small and can be neglected.

To reduce the computational time and to simplify the complete model, the aerodynamic loads are calculated by expressing the equations as Taylor-series-expansion (small angles of attack considered) for different propeller angular rate. The only not negligible aerodynamic loads are acting along Z-axis, i.e., the thrust and the reaction torque. The method presented in [19] has been used to verify that the only loads noteworthy are along Z-axis. Subsequently, torque and force varying with RPM were measured experimentally.

In the second equation of (14), the gyroscopic torque produced by the propeller can be found due to a rotating propeller that follows the rotations of the airframe. Note that for multirotors the gyroscopic terms produced by propellers are the dominant ones. This is a consequence of the high rotational speed in hovering (with respect to the gyroscopic term due to the body angular rates).

The components of the translational velocity V are expressed in (19), (20), and (21) where T_i for $i = 1, \ldots, 6$ is the i^{th} motor thrust. The variation of the angular velocity is expressed by (22), (23), and (24), where C_i for $i = 1, \ldots, 6$ is the i^{th} motor reaction torque and Ω is the total angular velocity of the propellers, d_1 is the distance from the motors $(1, 3, 4, 6)$ to the X_B axis, l_p is the distance between the motors $(3, 4)$ and the X_B axis, d_2 is the distance between the motors $(1, 3, 4, 6)$ and the Y_B axis, and d_3 is the distance between the CoM of the hexacopter and the Y_B axis considering geometrically unbalanced total mass of the hexacopter. Note that consideration of the location of the CoM of the hexacopter causes the different equation for $\dot{q}$ in (23) compared to those in [17], [18].

V. EXPERIMENTAL RESULTS

To validate the results of the parameters from the proposed identification method, flight experiments of the hexacopter are implemented. In the experiments, the hexacopter initially hovers on a desired position, and performs pitch and yaw accelerating movements. We, then, verify the nonlinear model and the parameters of identification using the equations (22), (23), and (24). The identified parameters are the moments of inertia, thrust computed from the PWM values of the engines based on (9), and the angular velocity of the propellers based on (8) and (9). For example, in the yaw acceleration experiment, we compare the measured pitch

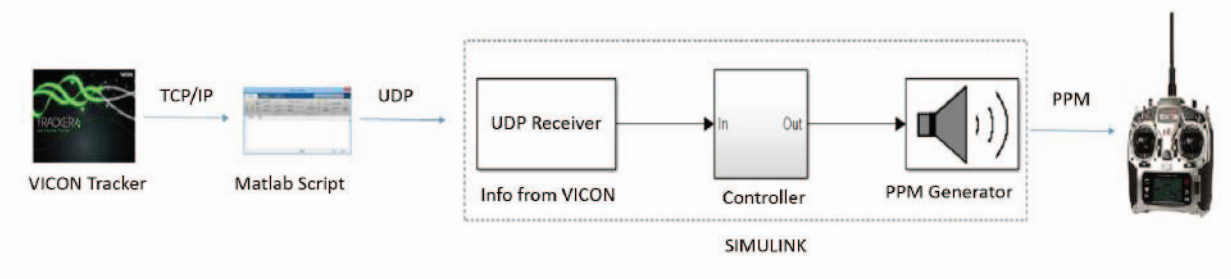

Fig. 14. Setup for flight experiments

acceleration value by the Vicon system with the computed value of (23) using identified parameters such as I_{yy}, thrust T_i estimated from the PWM, and Ω. Here, we use the measured angular velocity p and r to mitigate the difficulty in selecting initial values.

The basic setup for the flight experiments is as shown in Fig. 14. The Vicon system tracks the position and orientation of the hexacopter. A Matlab script then imports the data from the Vicon system to the ground station computer through a TCP/IP port and sends the data to a receiving block of a PID controller in Simulink environment through a UDP port. The PID controller provides control inputs to make the hexacopter hover at a desired position, move to specific direction, and change its attitude. PWM signals based on the control inputs are generated and packed into a pulse position modulation (PPM) frame. The PPM pulses are transmitted to the Pixhawk on the hexacopter by a DX7s transmitter. In the experiments, scheduled impulsive control inputs are generated for accelerating the angular movement of the hexacopter along a specific direction while it is hovering.

In the pitch acceleration case, impulsive inputs are applied to generate pitch acceleration at 10.2 s and 22.2 s while the hexacopter hovers. Fig. 15 illustrates the time histories of the measured outputs from the Vicon system and the estimated values using the parameters and the nonlinear equation (23). The estimated values are overall well-correlated to the measured acceleration.

Similarly, the yaw acceleration experiment is implemented. The moment of inertia I_{zz} is validated by comparing the estimated from (24) value with the measured acceleration. Fig. 16 shows the time histories of the estimated and measured yaw acceleration values. At the positive acceleration peaks, the estimated value is slightly smaller than the measured value. When negative impulsive inputs are applied, however, the acceleration values are well-matched.

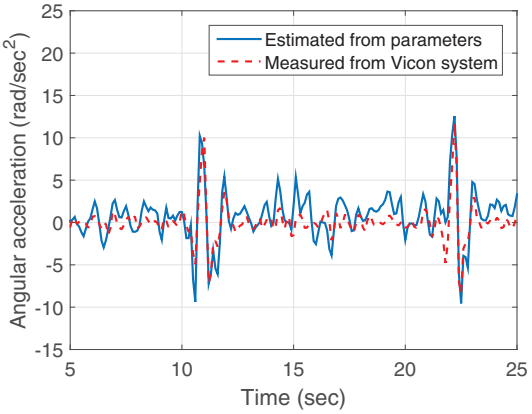

Fig. 15. Pitch acceleration

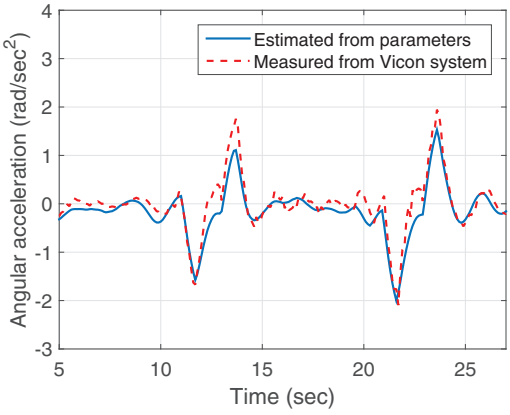

Fig. 16. Yaw acceleration

Thus, the effectiveness of the identification method and nonlinear dynamic model are validated through the flight experiments.

VI. CONCLUSIONS

In this paper we proposed a method to identify parameters of a multicopter in order to obtain a precise nonlinear model. A compound pendulum and an optical position tracking system have been utilized to obtain the values of the parameters of the multicopter such as the moments of inertia, the thrust and the torque of each motors. The identification method is computationally simpler than the approach of direct computation of geometry. It is also a low-risk method including a unique way to measure thrust and torque generated by propellers without possible damages during flight tests before understanding exact characteristics of the multicopter. A nonlinear model of the hexacopter was derived and the values of the parameters in the nonlinear model were validated by the data from the flight experiments. We have shown that the acceleration estimated by the parameters are closely matched the measured values in the experiments. The paper demonstrates that the proposed identification method is effective and supports further development of advanced controllers for multicopters.

ACKNOWLEDGMENT

This material is partially based upon work supported by the Air Force Office of Scientific Research, Air Force Material Command, USAF under Award No. FA2386-14-1-5007.

REFERENCES

[1] A. Chovancová, T. Fico, L. Chovanec, and P. Hubinsk, "Mathematical Modelling and Parameter Identification of Quadrotor (a survey)," *Procedia Engineering*, vol. 96, pp. 172-181, 2014.

[2] X. Zhang, X. Li, K. Wang, and Y. Lu, "A Survey of Modelling and Identification of Quadrotor Robot," *Abstract and Applied Analysis*, vol. 2014, 2014.

[3] N. Abas, A. Legowo, and R. Akmeliawati, "Parameter identification of an autonomous quadrotor," *4th International Conference On Mechatronics (ICOM)*, pp. 1-8, 2011.

[4] M. Elsamanty, A. Khalifa, M. Fanni, A. Ramadan, and A. Abo-Ismail, "Methodology for identifying quadrotor parameters, attitude estimation and control," *IEEE/ASME International Conference on Advanced Intelligent Mechatronics (AIM)*, pp.1343-1348, 2013.

[5] I. Stanculeanu and T. Borangiu, "Quadrotor black-box system identification," *World Academy of Science, Engineering and Technology*, vol. 78, 2011.

[6] W. Gracey, "The experimental determination of the moments of inertia of airplanes by a simplified compound-pendulum method," *NACA-TN-1629*, NASA, 1948.

[7] S. Patankar, D. Schinstock, and R. Caplinger, "Application of pendulum method to UAV momental ellipsoid estimation," *6th AIAA Aviation Technology, Integration and Operations Conference (ATIO)*, 2006.

[8] K. Bergman and J. Ekström, "Modeling, Estimation and Attitude Control of an Octorotor Using PID and $\mathcal{L}_1$ Adaptive Control Techniques, " *Master's Thesis*, University of Linköping, 2014.

[9] G. Szafranski, R. Czyba, and M. Blachuta, "Modeling and identification of electric propulsion system for multirotor unmanned aerial vehicle design," *2014 International Conference on Unmanned Aircraft Systems (ICUAS)*, May 27-30, Orlando, FL, 2014.

[10] F. Beltramini, M. Bergamasco, and M. Lovera, "Experiment design for MIMO model identification, with application to rotorcraft dynamics," *18th IFAC World Congress*, vol. 18, pp. 14392-14397, 2011.

[11] T. Magnusson, "Attitude Control of a Hexarotor," *Master's Thesis*, University of Linköping, 2014.

[12] M. Z. Rafat, M. S. Wheatland, and T. R. Bedding, "Dynamics of a double pendulum with distributed mass, " *American Journal of Physics*, vol. 77, pp. 216-223, 2009.

[13] S. Bouabdallah, "Design and Control of Quadrotors with Application to Autonomous Flying, " *PhD dissertation*, cole polytechnique fdrale de Lausanne, 2007.

[14] M. Ciarcià, A. Grompone, and M. Romano, "A near-optimal guidance for cooperative docking maneuvers," *Acta Astronautica*, vol. 102, pp. 367-377, 2014.

[15] J.S. Hall and M. Romano, "Laboratory Experimentation of Guidance and Control of Spacecraft During On-orbit Proximity Maneuvers," *Mechatronic Systems Simulation Modeling and Control*, A. Milella, D. Di Paola, and G. Cicirelli, Rijeka, Croatia:InTech, 2010, Ch. 11, pp. 187-225, 2010.

[16] B. Etkin and L. Reid, *Dynamics of Flight: Stability and Control*, New York: John Wiley and Sons (3^{rd} edition), 1996.

[17] R. Baránek and F. Šolc, "Modelling and control of a hexacopter," *2012 International Carpathian Control Conference (ICCC)*, 2012.

[18] D. Derawi, N. Salim, M. Rahman, S. Maxlan, and H. Zamzuri, "Modeling, attitude estimation, and control of hexarotor micro aerial vehicle ('MAV')," *2014 International Conference on Industrial Technology (ICIT)*, Busan, Korea, Feb. 26-Mar. 1, 2014.

[19] O. Flachsbart and G. Krober, *Experimental investigation of aircraft propellers exposed to oblique air currents*, NASA Technical Report, 1929.